13 December 1996

ELSEVIER

Chemical Physics Letters 263 (1996) 521-529

CHEMICAL PHYSICS LETTERS

Dielectric response of solvent surrounding an ion pair: Ewald potential versus spherical truncation

Gabriela S. Del Buono, Francisco E. Figueirido, Ronald M. Levy

Department of Chemistry, Rutgers, The State University of New Jersey, Piscataway, NJ 08855, USA

Received 17 May 1996; in final form 15 October 1996

Abstract

The solvent dielectric response has been evaluated for a system of two oppositely charged ions in aqueous solution. When the Ewald potential is used to model the long-range interactions, the correct high dielectric shielding of the ions by the water is obtained by either of two methods; from the ion charging free energies, or the slope of the ion–ion potential of mean force in the asymptotic region. In contrast, simply truncating the Coulomb interactions leads to unphysical dielectric behavior.

1. Introduction

The treatment of electrostatic interactions in simulations of charged species in polar solvents is difficult due to the long-range character of the Coulombic potential. Often, the electrostatic interactions are simply truncated in order to reduce the computational requirements. However, truncation of the electrostatic interactions can introduce artifacts [1–8]. For instance, quantities such as the dielectric constant which are strongly dependent on the solvent orientational structure are not accurately reproduced. Other examples of problems arising from truncation of the long-range electrostatic interactions include incorrect estimates of the stability of protein helices in aqueous solution [3], the energetics of peptides in ionic solutions [2], and the dynamics of simple solutes in solution [9].

Renewed attention is being focused on analyzing the effects of different truncation schemes on simulations of the thermodynamic and dynamic properties of inhomogeneous systems. For example, Bader and Chandler found that a smooth spherical truncation of the electrostatic interactions in a system of ferrous–ferric ions in aqueous solution introduced an unphysical attraction between the ions at relatively large separations [1]. When the long-range electrostatic interactions were calculated with the Ewald summation method, this artifact was removed; for this latter case, their calculated potential of mean force approached the expected dielectric continuum limit at large ion–ion separations. Earlier studies of a sodium dimethylphosphate system in solution showed repulsion of the oppositely charged ions at long distances; this behavior was also attributed to the use of spherical truncation [10,8]. Conflicting results regarding the first minimum of the potential of mean force have been found for studies on a Cl^- pair in solution [11–14]. Two studies employing spherical truncation [12,11] predicted the existence of deep minimum wells at short but different Cl^-–Cl^- separations. Dang and Pettitt [12] observed a stable contact ion pair, whereas Buckner and Jorgensen [11] predicted a stable solvent-separated ion pair.

These results disagree with those reported by Guardia et al. [13] and Hummer et al. [14] in which

PII S0009-2614(96)01234-1

no evidence for anion pairing was found, although they did report a very weak solvent separated minimum. Both of the groups used the Ewald potential. In addition, Hummer et al. [14] performed analogous studies using two different water models, as well as using reaction field techniques; all of their results were consistent with those obtained using the Ewald potential.

Recently, we reported calculations of the intrinsic pKa shifts of titratable groups in lysozyme [15]. The calculations were based on the free energy changes occurring upon ionization of the titratable groups. The calculated pKa shifts of several titratable residues were significantly larger than expected. Also the estimated dielectric shielding between pairs of charged residues was smaller than expected. Evidence was presented that suggested the truncation of the electrostatic interactions was at least partially responsible for the differences. In contrast, recent studies on a simple dicarboxilic acid in solution using the Ewald summation have yielded pKa shifts that are consistent with experimental results [16]. These observations, in addition to work by other groups, prompted the present analysis of solvent dielectric screening of ionic interactions. The dielectric screening by solvent observed in simulations employing the Ewald potential are compared with the results of simulations which employed truncated Coulomb potentials.

The solvent dielectric response for a relatively simple system of two oppositely charged chloride-like ions in aqueous solution was studied. The dielectric response was calculated using two approaches. In the first approach, the solvent dielectric response was obtained by calculating the free energy difference of charging the two ions at finite and infinite separation. In the second approach, dielectric constant estimates were obtained by monitoring the dependence of the ion–ion mean force on the interionic separation. The two methods can be used to form a thermodynamic cycle. The results from simulations performed using spherical truncation methods are compared to those with the Ewald potential. In Section 2, we outline the formalism behind each approach and give the details of molecular dynamics simulations. The results are presented and discussed in Section 3; differences between the truncated Coulomb and Ewald potentials are also analyzed. In Section 4 we summarize the results and present our conclusions.

2. Methods

2.1. Free energy calculations

The solvent dielectric response in a system of two ions in solution can be obtained from free energy calculations by two different paths. These two approaches are related through a simple thermodynamic cycle (see Fig. 1). One of them relates the solvent dielectric response to the free energy difference of charging the two ions at finite and infinite separation (Paths 1 and 3 in the cycle) [1]. The second approach relates the dielectric constant to the slope of the ion–ion potential of mean force in the asymptotic region (Path 2). The thermodynamic cycle can be closed by integrating the potential of mean force to obtain the solvation free energy difference between ions at infinite and finite separation. Alternatively, as in this communication, the dielectric constant can be estimated by directly monitoring the mean force on the solutes at different ion–ion separations in the asymptotic region.

The formalism for the two paths which are referred to here as the Potential and Force routes is presented in the following sections.

2.1.1. The potential route

The first approach is based on the following equation:

$$\Delta\Delta A = q_1 q_2 \frac{\Phi(x_1 - x_2)}{\varepsilon}. \tag{1}$$

For the case of two particles that are oppositely charged $\Delta\Delta A = \Delta A_1 - \Delta A_3$ (see Fig. 1); with $\Delta A_1 = A(+1,-1) - A(0,0)$, and $\Delta A_3 = (A(0,-1) - A(0,0)) + (A(+1,0) - A(0,0))$. Φ represents the direct electrostatic interaction between the ions.

The free energy of charging a single ion immersed in the solvent is given by

$$\Delta A = \int_{q_i}^{q_f} \mathrm{d}q \, \langle \phi_{\mathrm{solv}}(x_\alpha) \rangle_q, \tag{2}$$

[1] In the case of ions at infinite separation the free energy of charging the ions can be approximated by adding the free energies of charging each of the ions separately, while leaving the charge in the other ion set to zero. Any dependence on the cavity produced by the other ion can be assumed to be negligible at the large ion–ion separations considered here.

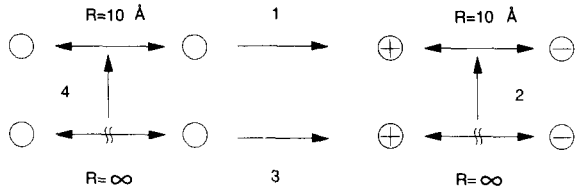

Fig. 1. Thermodynamic cycle.

where ϕ_{solv} is the electrostatic potential at the ion site due to the solvent. This formula can be easily extended to the case of two ions in solution. If the charging process obeys linear response, then the mean values ϕ_{solv} are linear in q and the free energy difference between charging both ions at finite and infinite separation can be written in terms of the mean values at the end points. In that case, the expressions would be given by

$$\Delta A_3 = \tfrac{1}{2}(\langle \phi_{\mathrm{solv}}(\boldsymbol{x}_+)\rangle_+ - \langle \phi_{\mathrm{solv}}(\boldsymbol{x}_-)\rangle_-), \tag{3}$$

$$\Delta A_1 = \tfrac{1}{2}(\langle \phi_{\mathrm{solv}}(\boldsymbol{x}_+) - \phi_{\mathrm{solv}}(\boldsymbol{x}_-)\rangle_{+,-}) - \Phi(\boldsymbol{x}_+ - \boldsymbol{x}_-). \tag{4}$$

In our study, the averaged potentials varied linearly with the charge (i.e., the ion charging followed the linear response formula, see Section 3.1). Once the free energy differences are evaluated the dielectric constant can then be obtained from the following equation,

$$\Delta\Delta A = \tfrac{1}{2}\Delta\Delta\langle \phi_{\mathrm{solv}}(\boldsymbol{x}_+, \boldsymbol{x}_-)\rangle - \Phi(\boldsymbol{x}_+ - \boldsymbol{x}_-) = -\frac{\Phi(\boldsymbol{x}_+ - \boldsymbol{x}_-)}{\varepsilon}, \tag{5}$$

where

$$\Delta\Delta\langle \phi_{\mathrm{solv}}(\boldsymbol{x}_+, \boldsymbol{x}_-)\rangle = \langle \phi_{\mathrm{solv}}(\boldsymbol{x}_+) - \phi_{\mathrm{solv}}(\boldsymbol{x}_-)\rangle_{+,-} - \langle \phi_{\mathrm{solv}}(\boldsymbol{x}_+)\rangle_+ + \langle \phi_{\mathrm{solv}}(\boldsymbol{x}_-)\rangle_-). \tag{6}$$

The expression contained in Eq. (6) is obtained from molecular dynamics simulations.

The electrostatic potentials are calculated using the standard Ewald expression for a system surrounded by a conductor [20],

$$\Phi_{\mathrm{Ew}}(\boldsymbol{x}) = \sum_{\boldsymbol{n}\in\mathbb{Z}^3} \frac{\operatorname{erfc}(\alpha\|\boldsymbol{x} - L\boldsymbol{n}\|)}{\|\boldsymbol{x} - L\boldsymbol{n}\|} + \frac{1}{\pi}\sum_{\boldsymbol{k}\in\mathbb{Z}^3,\boldsymbol{k}\neq\boldsymbol{0}} \frac{\exp\left(-\pi^2\frac{\|\boldsymbol{k}\|^2}{\alpha^2L^2} + \frac{2\pi\mathrm{i}}{L}\langle \boldsymbol{x}, \boldsymbol{k}\rangle\right)}{L\|\boldsymbol{k}\|^2} - \frac{1}{L}\frac{\pi}{(\alpha L)^2}, \tag{7}$$

where L is the size of the unit cell.

2.1.2. The force route

The second approach to calculating the solvent dielectric response monitors the mean force on the solutes as the separation, r, between the two charged ions is varied. The potential of mean force, $W(r)$, can be related to the mean forces. The derivative of $W(r)$ with respect to r gives the mean force between the ions, $F(r)$,

$$F(r) = -\frac{\mathrm{d}}{\mathrm{d}r}W(r) = F_0(r) + \Delta F(r). \tag{8}$$

$F_0(r)$ is the direct solute–solute force (i.e., in the absence of solvent), and $\Delta F(r)$ is the solvent-averaged contribution.

At large r the solvent reduces the direct Coulombic interaction by a factor of the bulk dielectric constant. Thus in the continuum limit, Eq. (8) becomes

$$F(r) \approx \frac{F_0(r)}{\varepsilon}. \tag{9}$$

The only forces affecting ε in the continuum regime are the mean electrostatic forces; therefore in calculating the dielectric constant, the Lennard-Jones forces were ignored and only the mean electrostatic forces were included.

2.2. Computer simulation

Using the IMPACT computer program [17], Molecular Dynamics (MD) simulations were carried out on systems comprised of two chloride-like solutes immersed in either 417 or 1103 SPC [18] water molecules. The ion charging states and interionic separations are listed in Table 1.

The equations of motion were integrated using Andersen's RATTLE algorithm with a timestep of 1 or 2 fs [17,19]. The solutes were held at a fixed distance

Table 1
Overview of simulations

q (au)	N_{H_2O}	$r_{ion\text{-}ion}$ (Å)	Truncation	Timestep (fs)	Time (ps)
+1.0,−1.0	1103	10	Ewald	1	200
+0.5, −0.5	1103	10	Ewald	1	200
+1.0, 0.0	1103	10	Ewald	1	200
+0.5, 0.0	1103	10	Ewald	1	200
0.0, −1.0	1103	10	Ewald	1	200
0.0, −0.5	1103	10	Ewald	1	200
0.0, 0.0	1103	10	Ewald	1	100
+1.0, −1.0	1103	9	Ewald	1	100
+1.0, −1.0	1103	8	Ewald	1	100
+1.0, −1.0	1103	10	r_c = 14 Å	1	200
+1.0, −1.0	1103	9	r_c = 14 Å	1	100
+1.0, −1.0	1103	8	r_c = 14 Å	1	100
+1.0, −1.0	1103	8	r_c = 8 Å	1	100
+1.0, −1.0	1103	8	r_c = 11.73 Å	2	80
+1.0, −1.0	1103	8	r_c = 16 Å	2	100
+2.0, +3.0	417	8	r_c = 11.73 Å	2	200
+2.0, +3.0	417	8	r_c = 11.73 Å,smooth	2	200
+1.0, −1.0	417	8	r_c = 11.73 Å	2	200
+1.0, −1.0	417	8	r_c = 11.73 Å,smooth	2	80

during the simulations; this constraint was enforced by setting the forces on each solute to zero at each time step. The density of the systems was approximately 1 g/cm^3, corresponding to cubic cells of length 24.36 Å and 32 Å. The usual periodic boundary conditions were implemented.

Several related molecular dynamics simulations were carried out (see Table 1). Ewald summation [20,21] and spherical truncation were applied to both the water–water and water–ion interactions. A non-bonded list was regenerated every 5 fs. The Ewald convergence parameter, α, was set to $5.5/L$, where L is the cubic cell length; the reciprocal space portion of the Ewald potential was evaluated using $k = 5$, with $k^2 < 14$.

The non-electrostatic part of the ion–water potential was a chloride Lennard-Jones 6–12 potential with parameters given by Jorgensen et al. [22]. The temperature was fixed at 298 K using Berendsen's scaling method with a relaxation time of 0.01 ps [23].

Table 1 shows the length of the simulations for the different systems. For each simulation the system was allowed to equilibrate between 40 and 80 ps before the production runs were performed. Configurations were stored every 100 fs for subsequent analysis.

3. Results and discussion

In Sections 3.1 and 3.2, the solvent dielectric responses calculated from the potential and force approaches using the Ewald method are reported and compared. In Section 3.3, the consequences of truncating the electrostatic interactions in MD simulations are examined. The mean forces obtained with the truncated Coulomb interactions are then compared to those evaluated using the Ewald summation method.

3.1. Charging free energy

Fig. 2a shows the running average of the difference in electrostatic potentials due to the solvent between systems of one and two fully charged ions (see Eq. (6)); the potentials have apparently converged after 200 ps of simulation.

In Fig. 3 we show $\Delta\Delta\langle\phi_{solv}(\boldsymbol{x}_+, \boldsymbol{x}_-)\rangle$ (see Eq. (6)) with respect to the charging state. Error bounds on the potentials are estimated using Eq. (11).

The linear dependence of the difference in the average electrostatic potentials with respect to the charging state is seen in Fig. 3. This observed linearity permits the direct evaluation of the free energy difference (see Eq. (5)).

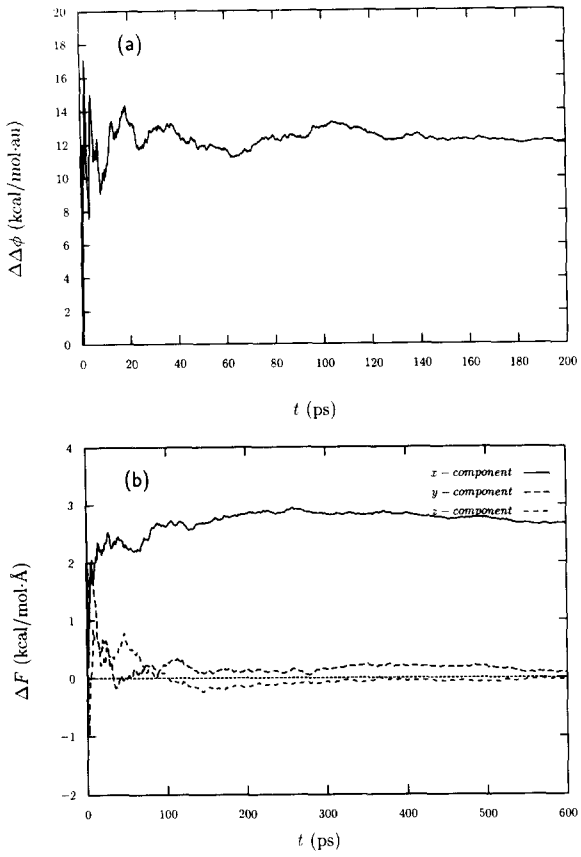

Fig. 2. (a) Running average of the difference in electrostatic potentials due to the solvent for the fully charged ions, $\Delta\Delta\langle\phi_{\mathrm{solv}}(x_+, x_-)\rangle$ (see Eq. (6)). (b) Running average of the x, y and z components of the solvent averaged contribution to the mean force between the ions at 10 Å separation, ΔF (see Eq. (8)).

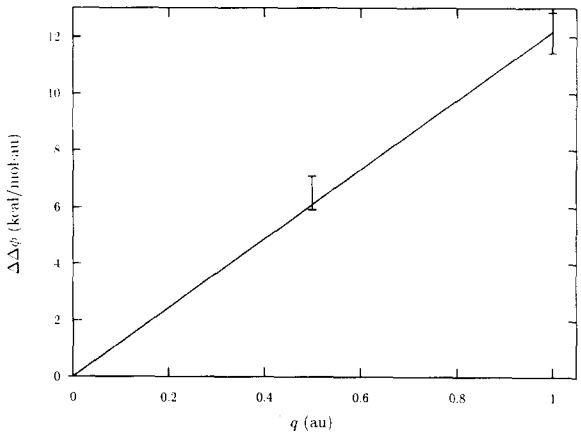

Fig. 3. Difference in average electrostatic potentials, $\Delta\Delta\langle\phi_{\mathrm{solv}}(x_+, x_-)\rangle$ (see Eq. (6)), with respect to the charging state. Statistical uncertainties were obtained using Eq. (11) (see Section 3.1); t_F's and $\sigma(F)$ for $q = 0.5, 1$ au are 0.1, 0.15 ps and 18, 19 kcal/mol respectively.

Behavior consistent with linear response theory was also obtained by Levy et al. [24,25] for the charging of two ions in solution up to a charging state of $0.7e$; non-linearities were observed beyond that point. The simulation length was short and spherical truncation was used; further work is required in order to establish whether the nonlinear behavior was an artifact of the truncation method used and/or statistical uncertainties. Hummer et al. [26] studied the hydration free energies of single ions in solution using the Ewald potential. They observed a linear dependence between the potential and the charge for both positively and negatively charged ions, but with a different slope.

The dielectric constant, ε is calculated using Eq. (5). The average value ε obtained by this scheme is 62, which is in very good agreement with the dielectric constant of SPC water. A lower bound for ε is approximately 8 for this case. From Eq. (5), the graph of $\Delta\Delta\langle\phi_{\mathrm{solv}}(x_+, x_-)\rangle$ versus ε is hyperbolic. Because the values of $\Delta\Delta\langle\phi_{\mathrm{solv}}(x_+, x_-)\rangle$ found in this calculation lie near the asymptote of the hyperbola, the values of the dielectric constant extracted from the graph are sensitive to small changes in $\Delta\Delta\langle\phi_{\mathrm{solv}}(x_+, x_-)\rangle$. For instance, a 6% change in $\Delta\Delta\langle\phi_{\mathrm{solv}}(x_+, x_-)\rangle$ causes an 87% change in the dielectric constant. While it is difficult to determine ε with high precision by the thermodynamic route (Eq. (5)), this is the method which most directly probes the dielectric properties of the ions/solvent free energy surface.

The direct interaction portion of the Ewald potential energy, $-\Phi(x_+ - x_-)$, is -6.2 kcal/mol for the two ions separated by 10 Å. The difference between the direct Ewald potential (6.2 kcal/mol) and the potential predicted by Coulomb's law for two charges 10 Å apart in vacuum (33.2 kcal/mol) arises primarily from a shifting of the Ewald potential in a periodic system relative to the Coulomb potential in an infinite system. This shift introduces a volume dependence that is not negligible. This issue is addressed in detail by Figueirido et al. in a related paper [21].

3.2. Mean electrostatic forces

The average electrostatic force $F(r)$ was calculated for the ionic separations given in Table 1. The solvent forces acting on the ions are projected onto the vector between the ions. The average of these projections is related to the mean electrostatic force by the following equation,

$$F(r) = \tfrac{1}{2}\langle(\boldsymbol{F}_{\mathrm{Cl}^+} - \boldsymbol{F}_{\mathrm{Cl}^-}) \cdot \hat{\boldsymbol{r}}\rangle + F_0(r). \qquad (10)$$

The ratio $F(r)/F_0(r)$ is expected to be inversely proportional to ε (see Eq. (9)) for sufficiently large r. Since the ions are constrained to the x-axis, then by symmetry, the y and z components of the time averaged solvent fluctuating force ($\Delta F(r)$, see Eq. (8)) approach zero. The time evolution of the parallel and perpendicular components of ΔF are shown in Fig. 2b. The perpendicular components approach zero rapidly, while the parallel component approaches a value which essentially cancels the direct ion–ion force. All the components exhibit a small amplitude long wavelength oscillation which dominates the error in the estimates of the mean values.

In Fig. 4a, we show the ratio of the forces when using the Ewald potential. The data corresponding to ionic separations of 9 Å and 10 Å in this figure were obtained from longer MD simulations than those reported in Table 1 (500 and 600 ps respectively); the motivation for the longer simulations was based on attempting to reduce the error bars. Final results show that the asymptotic region of the curve is consistent with the value of $\varepsilon \approx 68$ found in SPC water models.

Small force ratios correspond to high dielectric shielding of the interionic interactions . Physically, this implies the direct ionic forces are largely canceled by the fluctuating solvent forces. These results are in agreement with previous calculations of the mean electrostatic forces on a ferrous–ferric system in solution [1]. Thus, this method and the charging free energy method are consistent and give the expected dielectric response for the solvent.

Error bounds on the mean forces and average potentials were estimated using Eq. (11) [20]:

$$\sigma^2(\langle F\rangle) \approx \frac{2t_F\sigma^2(F)}{t}, \qquad (11)$$

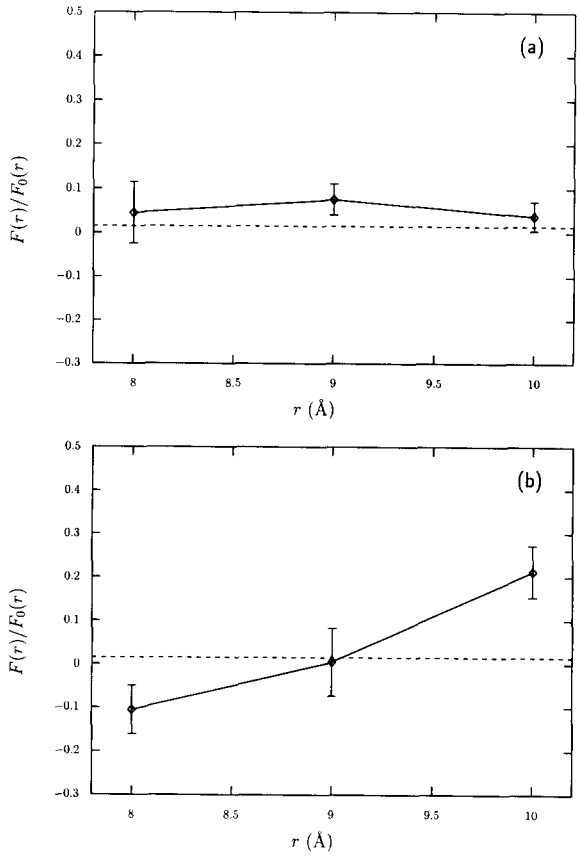

Fig. 4. Mean force ratio ($F(r)/F_0(r)$) between two oppositely charged chloride-like ions in water computed from simulations using different truncation schemes; (a) the Ewald sum method, (b) spherical truncation at 14 Å. The dashed line is the continuum limit with $\varepsilon = 68$. Statistical uncertainties for the simulations were obtained using Eq. (11) (see Section 3.1). For (a), t_F's and $\sigma(F)$ for $r = 8, 9, 10$ Å are 0.27, 0.31, 0.2 ps and 0.8, 1.0, 1.3 respectively; for (b), t_F's and $\sigma(F)$ for $r = 8, 9, 10$ Å are 0.32, 0.35, 0.3 ps and 0.7, 0.94, 1.1 respectively.

where t_F is the decorrelation time of the calculated quantity, and t the total simulation time.

This equation is based on the assumption that the time necessary to obtain statistically independent samples is approximately equal to the decorrelation time of the autocorrelation function of the quantity being evaluated. An estimate of the decorrelation time is obtained from graphs of the autocorrelation function of the electrostatic force (see Eq. (10)) versus time. From the resulting error bounds for the statistics obtained here, a lower bound for ε is approximately 14.

3.3. Mean electrostatic forces using a truncated Coulomb potential

The force ratios $F(r)/F_0(r)$ obtained from simulations using a 14 Å cutoff radius were compared to those obtained from simulations using the Ewald method. The results are shown in Fig. 4b. The figure shows that the truncation method does not yield the correct continuum asymptotic result for the mean forces. The forces obtained with the truncation method suggest the existence of an attractive well for the potential of mean force, with a minimum close to 9 Å. The mean force at the largest separation studied, r = 10 Å, corresponds to a dielectric constant that is positive, but small in magnitude ($\varepsilon \approx 5$); hence, relatively low dielectric shielding is observed for this case. This result is consistent with our previous studies on lysozyme in solution using truncation [15].

Comparisons were also made of the effects of abrupt and smooth truncation of the interactions on the mean forces. Two systems were examined: Cl^-/Cl^+, and Fe^{2+}/Fe^{3+} in solution. Simulation conditions similar to those used by Bader and Chandler in their ferrous–ferric ions system were employed [1] (see Table 1). For the non-electrostatic part of the potential in the ferrous–ferric ion case, a Lennard-Jones 6–12 potential was employed (σ = 3.3447 Å, ϵ = 0.008929 kcal/mol). The parameters were obtained by finding the best fit to the $1/r^9$ type potential used by Bader and Chandler in their model. A quintic spline was used as a smoothing function, instead of the cubic spline used by Bader and Chandler. The results are shown in Table 2. The mean force obtained for the ferrous-ferric ions system using smooth truncation is in excellent agreement with calculations by Bader and Chandler [1] (we estimated $F(r)$ to be −8 kcal/mol Å in their case). Several observations can be made from these results. For both systems the behavior of the mean forces is inconsistent with the expected dielectric continuum limit; at large ionic separations, attractive forces are observed for the like-charged ion pair system and vice versa for the oppositely charged ion pair system. This effect is magnified in both systems when smooth truncation is used.

We also tested whether the results obtained with increasing interaction cutoff converge to the Ewald results. The mean electrostatic forces for the chloride-like ions system were calculated from simulations performed using different cutoff radii; the interionic separation was 8 Å for the examined cases. The results are shown in Fig. 5. The only quantity that changes is the solvent-ion force, ΔF (see Eq. (8)). Initially, ΔF is small; however, as the cutoff is increased to about 11 Å, ΔF increases until it nearly cancels the direct ion-ion force. For larger cutoffs ΔF is larger than the direct interaction. Physically, this implies the solvent dielectric response varies from very low dielectric shielding for low cutoffs to high shielding for a cutoff near 11 Å and for larger cutoffs becomes anti-shielding. Similar observations were made for the ferrous–ferric ions system (results not shown).

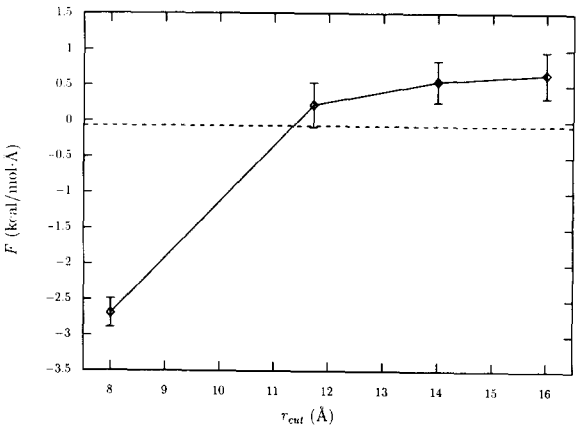

Fig. 5. Mean electrostatic force between two oppositely charged chloride-like ions separated by 8 Å in water in simulations using different cutoff radii r_{cut} to truncate the electrostatic interactions. The dashed line is the continuum limit result with ε = 68.

Table 2
The mean electrostatic force between two solutes 8 Å apart in solution using smooth and abrupt truncation. The cutoff radius is 11.73 Å (forces in kcal/mol Å)

System	Abrupt	Smooth (Δ = 0.5 Å)	Continuum (ε = 68)
Cl^-/Cl^+	0.39(0.2)	1.2(0.3)	−0.070
Fe^{2+}/Fe^{3+}	−1.8 (0.2)	−9.4(0.2)	0.46

4. Conclusions

The accurate calculation of the solvent dielectric response in a system of two charged particles is an important benchmark for any long-range interaction

model. Ewald sums have thus far given physically reasonable and consistent results [1,13]. Here, the solvent dielectric response was estimated for a system of two oppositely-charged ions using the Ewald summation method to evaluate the electrostatic interactions. Two approaches were used to perform the calculations. For both paths, the calculated dielectric constant was in good agreement with the expected high dielectric shielding.

In contrast, results obtained using spherical truncation gave a net repulsive interaction between the oppositely charged ions at relatively large separations (r = 8 Å). This behavior is unphysical and is most likely an artifact arising from the truncation of the interactions. As the interaction cutoff is increased the mean forces do not converge to a small and negative value as expected, but rather approach a non-negligible positive value; physically this translates into the solvent enhancing the interaction between the two ions. While a cutoff radius of about 11 Å gave a physically meaningful result, this is probably fortuitous since the calculated dielectric constant at larger cutoffs did not converge to this value. The problems appear to be independent of the actual implementation of the truncation. Both abrupt and smooth truncation gave unphysical results, with smooth truncation amplifying the unphysical contributions. Artifacts produced by smooth truncation methods on dynamical and structural properties of homogeneous and heterogeneous systems have also been recognized by other groups [27,28,9].

Recent pKa calculations on succinic acid in aqueous solution have shown that using the Ewald potential yields pKa shifts that are consistent with experiment [16]. The importance of conformational averaging on such calculations was also illustrated.

Although the Ewald potential yields accurate and consistent results for the solvent dielectric response of simple systems like ion pairs in water, other important issues need to be addressed. For example, what artifacts are introduced by the finite-size of the systems; this issue is discussed by Figueirido et al. [21]. Another concern is whether the number of solvent molecules currently feasible for simulations of biological systems is large enough to produce the correct bulk solvent effects in these complex heterogeneous systems. In this regard, systematic studies of size dependence are in order [26]. For the study of larger systems it is necessary to implement more efficient methods. A promising approach is to combine fast methods for the computation of the electrostatic interactions with efficient MD integrators [29].

Acknowledgement

This work has been supported in part by the National Institute of Health, Grant No. GM-30580 and by the National Science Foundation MetaCenter Allocation of Supercomputer Time.

References

[1] J.S. Bader and D. Chandler, J. Phys. Chem. 96 (1992) 6423.
[2] P.E. Smith and B.M. Pettitt, J. Chem. Phys. 95 (1991) 8430.
[3] H. Schreiber and O. Steinhauser, Chem. Phys. 168 (1992) 75.
[4] J.E. Roberts and J. Schnitker, J. Chem. Phys. 101 (1994) 5024.
[5] J.E. Roberts and J. Schnitker, J. Phys. Chem. 99 (1995) 1322.
[6] D.M. York, T.A. Darden and L.G. Pedersen, J. Chem. Phys. 99 (1993) 8345.
[7] C.L. Brooks, J. Chem. Phys. 86 (1987) 5156.
[8] R. Friedman and M. Mezei, J. Chem. Phys. 102 (1995) 419.
[9] G.S. Del Buono, T.S. Cohen and P.J. Rossky, J. Mol. Liq. 60 (1994) 221.
[10] S.E. Huston and P.J. Rossky, J. Phys. Chem. 93 (1989) 7888.
[11] J.K. Buckner and W.L. Jorgensen, J. Am. Chem. Soc. 111 (1989) 2507.
[12] L.X. Dang and B.M. Pettitt, J. Phys. Chem. 94 (1990) 4303.
[13] E. Guardia, R. Rey and J.A. Padro, J. Chem. Phys. 95 (1991) 2823.
[14] G. Hummer, D.M. Soumpasis and M. Neumann, Mol. Phys. 81 (1993) 1155.
[15] G.S. Del Buono, F.E. Figueirido and R.M. Levy, Proteins 20 (1994) 85.
[16] F. Figueirido, G.S. Del Buono and R.M. Levy, J. Phys. Chem. 100 (1996) 6389.
[17] D.B. Kitchen, F. Hirata, J.D. Westbrook, R.M. Levy, D. Kofke and M. Yarmush, J. Comput. Chem. 11 (1990) 1169.
[18] H.J.C. Berendsen, J.P.M. Postma, W.F. van Gunsteren and J. Hermans, Intermolecular forces (Reidel, Dordrecht, 1981).
[19] H.C. Andersen, J. Comput. Phys. 52 (1983) 24.
[20] M.P. Allen and D.J. Tildsley, Computer simulation of liquids (Oxford Univ. Press, Oxford, 1991).
[21] F. Figueirido, G.S. Del Buono and R.M. Levy, J. Chem. Phys. 103 (1995) 6133.
[22] W.L. Jorgensen, J.F. Blake and J.K. Buckner, Chem. Phys. 129 (1989) 193.
[23] H.J.C. Berendsen, J.P. Postma, W.F. van Gunsteren, A. DiNola and J.R. Haak, J. Chem. Phys. 81 (1984) 3684.
[24] R.M. Levy, M. Belhadj and D.B. Kitchen, J. Chem. Phys. 95 (1991) 3627.

[25] F. Figueirido, G.S. Del Buono and R.M. Levy, Biophys. Chem. 51 (1994) 235.
[26] G. Hummer, L.R. Pratt and A.E. Garcia, J. Phys. Chem. 100 (1996) 1206.
[27] P.J. Steinbach and B.R. Brooks, J. Comp. Chem. 15 (1994) 667.
[28] K.F. Lau, H.E. Alper, T.S. Thacher and T.R. Stouch, J. Phys. Chem. 98 (1994) 8785.
[29] F. Figueirido, R. Zhou, B.J. Berne and R.M. Levy, Large scale simulation of macromolecules in solution: combining the periodic fast multipole method with multiple time step integrators, J. Chem. Phys., submitted for publication.